AD-A032 116 AEROSPACE CORP EL SEGUNDO CALIF MATERIALS SCIENCES LAB F/G 20/8
THERMOLUMINESCENT DETECTOR SPECTRAL ANALYSIS ON THE RETRO-FOCUS--ETC(U)
OCT 76 G M MOLEN, K W PASCHEN, R H VANDRE F04701-76-C-0077
UNCLASSIFIED TR-0077(2250-20)-2 SAMSO-TR-76-215 NL

| OF |
AD
A032116

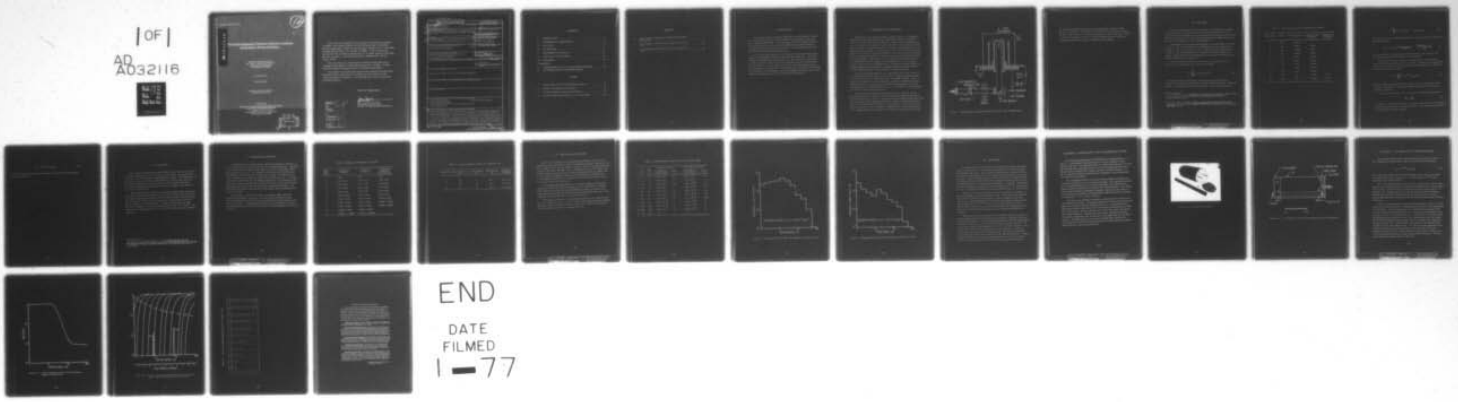

END

DATE
FILMED
1-77

REPORT SAMSO-TR-76-215

Thermoluminescent Detector Spectral Analysis on the Retro-Focus Simulator

Materials Sciences Laboratory
The Ivan A. Getting Laboratories
The Aerospace Corporation
El Segundo, Calif. 90245

22 October 1976

Interim Report

Prepared for

SPACE AND MISSILE SYSTEMS ORGANIZATION
AIR FORCE SYSTEMS COMMAND
Los Angeles Air Force Station
P.O. Box 92960, Worldway Postal Center
Los Angeles, Calif. 90009

This report was submitted by The Aerospace Corporation, El Segundo, CA 90245, under Contract F04701-75-C-0076 with the Space and Missile Systems Organization, Deputy for Advanced Space Programs, P.O. Box 92960, Worldway Postal Center, Los Angeles, CA 90009. It was reviewed and approved for The Aerospace Corporation by W. C. Riley, Director, Materials Sciences Laboratory. Lieutenant Jean Bogert, SAMSO/YAPT, was the Project Officer.

This report has been reviewed by the Information Office (OI) and is releasable to the National Technical Information Service (NTIS). At NTIS, it will be available to the general public, including foreign nations.

This technical report has been reviewed and is approved for publication. Publication of this report does not constitute Air Force approval of the report's findings or conclusions. It is published only for the exchange and stimulation of ideas.

FOR THE COMMANDER

Jean Bogert

Jean Bogert
1st Lt., U.S. Air Force
Technology Plans Division
Deputy for Advanced Space Programs

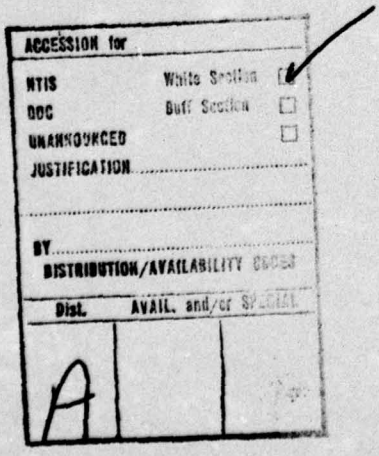

UNCLASSIFIED

SECURITY CLASSIFICATION OF THIS PAGE (When Data Entered)

REPORT DOCUMENTATION PAGE	READ INSTRUCTIONS BEFORE COMPLETING FORM
1. REPORT NUMBER: SAMSO-TR-76-215	2. GOVT ACCESSION NO. / 3. RECIPIENT'S CATALOG NUMBER
4. TITLE (and Subtitle): THERMOLUMINESCENT DETECTOR SPECTRAL ANALYSIS ON THE RETRO-FOCUS SIMULATOR	5. TYPE OF REPORT & PERIOD COVERED: Interim rept
	6. PERFORMING ORG. REPORT NUMBER: TR-0077(2250-20)-2
7. AUTHOR(s): G. Marshall Molen, Kenneth W. Paschen, Robert H. Vandre, Catherine T. Young	8. CONTRACT OR GRANT NUMBER(s): F04701-76-C-0077
9. PERFORMING ORGANIZATION NAME AND ADDRESS: The Aerospace Corporation, El Segundo, Calif. 90245	10. PROGRAM ELEMENT, PROJECT, TASK AREA & WORK UNIT NUMBERS
11. CONTROLLING OFFICE NAME AND ADDRESS: Space and Missile Systems Organization, Air Force Systems Command, Los Angeles, Calif. 90009	12. REPORT DATE: 22 October 1976
	13. NUMBER OF PAGES: 27 (12) 35 pp.
14. MONITORING AGENCY NAME & ADDRESS (if different from Controlling Office)	15. SECURITY CLASS. (of this report): Unclassified
	15a. DECLASSIFICATION/DOWNGRADING SCHEDULE

16. DISTRIBUTION STATEMENT (of this Report)

Approved for public release; distribution unlimited

17. DISTRIBUTION STATEMENT (of the abstract entered in Block 20, if different from Report)

18. SUPPLEMENTARY NOTES

19. KEY WORDS (Continue on reverse side if necessary and identify by block number)

Dense Plasma Focus
Retro-Focus Simulator
Thermoluminescent Detector (TLD) Dosimeters
X-Ray Diagnostics
X-Ray Spectral Analysis

20. ABSTRACT (Continue on reverse side if necessary and identify by block number)

A spectral analysis of the x-ray fluence from the Aerospace Mark IV plasma focus operated in the retro-focus mode is discussed. A dosimeter fixture with 11 thermoluminescent detectors was used to resolve the spectrum in the range of 1 to 1000 keV. Two x-ray converter materials, tantalum and aluminum, were studied to demonstrate spectral tailoring. The actual spectra were unfolded from experimental data by using an operator-implemented computer routine. An effective softening of the spectrum caused by the K-line emission at 1.5 keV was observed when the aluminum converter was used.

DD FORM 1473 (FACSIMILE)

UNCLASSIFIED

SECURITY CLASSIFICATION OF THIS PAGE (When Data Entered)

403 644

CONTENTS

TABLES

FIGURES

I. INTRODUCTION

A thermoluminescent detector (TLD) fixture was fabricated to resolve the x-ray spectrum from the Mark IV plasma focus operated in the retro-focus simulator (RFS) mode. The diagnostics were specifically designed to resolve the spectrum in the range of 1 to 1000 keV for various converter materials to demonstrate spectral tailoring. The technique has been used with both aluminum and tantalum converters.

Previous spectral analyses on the RFS were conducted by using combinations of transmitting foils and silicon PIN diode detectors. The diode response was proportional to the x-ray dose rate, unlike the TLDs, which are dose-dependent. The use of TLDs as dosimeters has two particularly attractive features: (1) the small physical size of the dosimeters permits the simultaneous irradiation of several TLDs, which minimizes experimental error from poor reproducibility, and (2) contributions from fluorescence and Compton scattering are more easily included in the analysis.

II. EXPERIMENTAL DESCRIPTION

The Mark IV retro-focus simulator is shown in Fig. 1. A significant modification of the conventional mode of operation is the use of a hollow-center electrode through which an energetic electron beam is transported to an x-ray converter by a copper drift tube extension. Thick targets of aluminum or tantalum are supported inside the converter housing to which a 1.4 m diagnostic tube is attached. Provision was made for the inclusion of an x-ray window between the housing and the diagnostic tube; however, these measurements were conducted without the window in order to avoid attenuation of the low-energy photons. High-energy electrons scattered from the converter were prohibited from entering the x-ray diagnostics by a 2.5 kG magnet oriented transverse to the diagnostic tube. A large aperture gate valve was installed adjacent to the diagnostics so that the dosimeter fixture could be removed without bringing the main chamber to ambient pressure.

Typical operating parameters were static fill pressures of 2.5 to 3.5 Torr deuterium and bank voltages of 12 to 16 kV. Higher charging voltages were not used because of concomitant risks of insulator damage. Experiments were conducted at a total capacitance of 168 μF in addition to several exposures at 84 μF. In order to accommodate the diagnostics, the device was operated in the grounded switch mode, i.e., the center electrode (anode) and attached drift tubes were grounded.

The Harshaw TLD-200 (CaF_2:Dy) dosimeters are mounted inside a 4.9 cm diam aluminum cylinder, which is described in detail in Appendix A. The fixture houses an array of 11 transmission filters affixed to the front of the package and their corresponding dosimeters, which are attached at the back plane. The TLD dosimeter crystals are square chips 3.2 mm on each side and 0.89 mm thick. The 11 TLDs were selected from a larger batch subject to the condition that, when exposed to a constant dose of soft or hard x-rays,

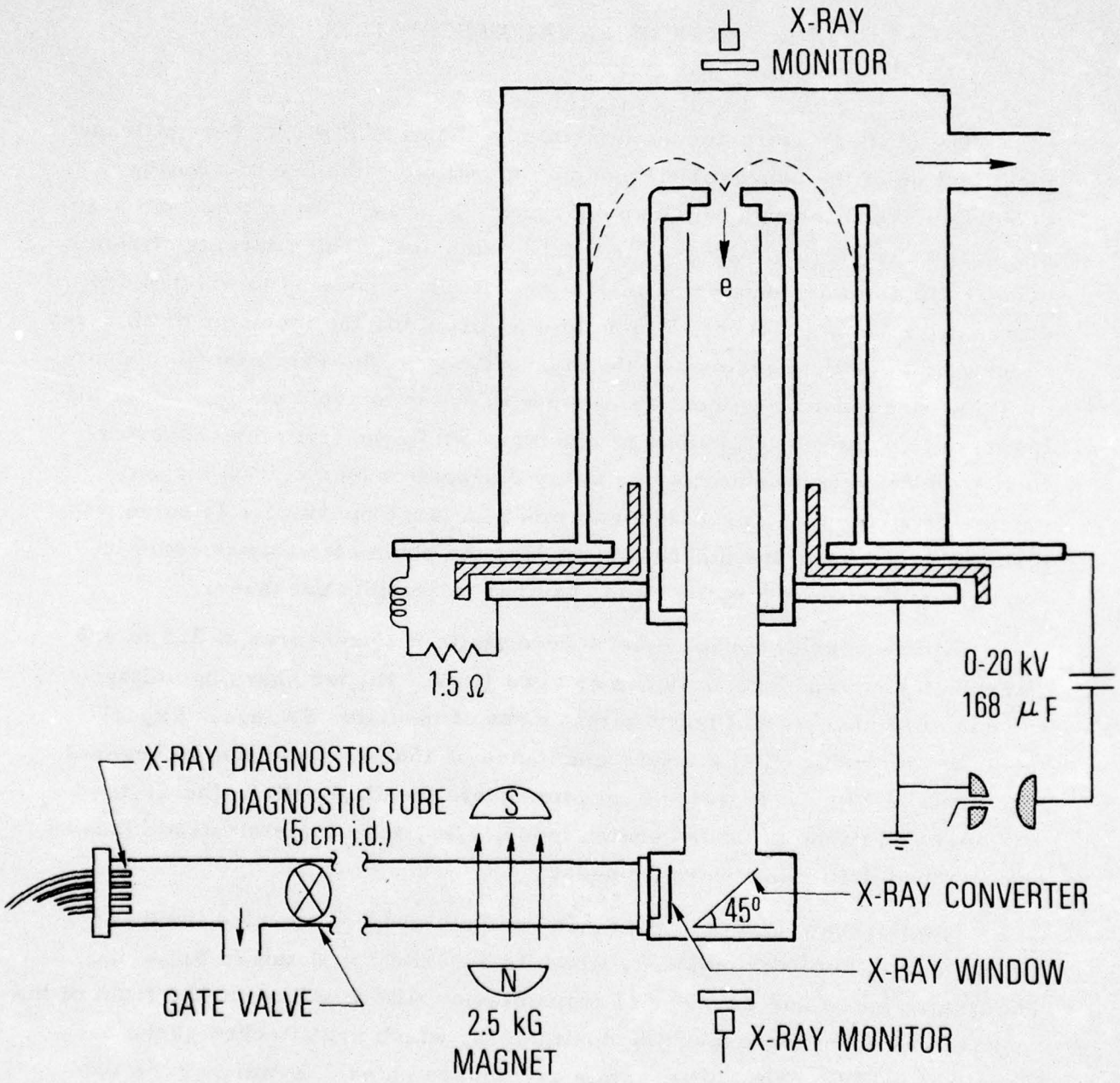

Figure 1. Experimental Arrangement of RFS Grounded Anode Configuration

the detectors exhibited shot-to-shot reproducibility in response to both spectra to within 2%. This aided in the elimination of TLDs that had imperfections, dirty surfaces, or different thicknesses, which would have resulted in erroneous readings. The less stringent condition that the TLDs have responses similar to each other was applied where possible.

III. ANALYSIS

The x-ray absorption of the TLD crystals was calculated by using the energy transfer cross section, which consists of the photoelectric cross section and the Klein-Nishina contribution (Compton absorption) to the energy transfer cross section.[1,2] The computed absorption for photon energies in the range of 1 to 1000 keV is given in Appendix B.

The filtration and the supporting windows used in the fixture are listed in Table 1. The corresponding x-ray transmission for each of the filters is shown in Fig. B-2, where each curve is indexed by the designation used in Table 1. The transmissions were computed by using the total cross section, which consists of the photoelectric cross section in addition to the total Klein-Nishina cross section.[1,2]

At a given distance from the x-ray source, the fluence $\mathcal{F}$ can be expressed as a summation over N intervals such that

$$\mathcal{F} \equiv \sum_{j=1}^{N} F_j \, \Delta E_j \quad \text{cal/cm}^2 \tag{1}$$

where F_j is the differential fluence of each interval in dimensions of cal/cm^2-keV, and ΔE_j is the width of each energy interval in keV. Thus, the dose G_i received by a TLD that is behind filter i can be represented as

---

[1] W. H. McMaster et al, Compilation of X-Ray Cross Sections, UCRL 50174, Sec. II, Rev. I, Lawrence-Livermore Laboratories, Livermore, California (May 1969).

[2] F. Biggs and R. Lighthill, Analytical Approximations for X-Ray Cross Section II, SC-RR-71 0507, Sandia Laboratories, Albuquerque, New Mexico (December 1971).

Table 1. X-Ray Filters used in TLD Dosimeter Fixture

Filter Index, i	Filter	Filter Thickness, cm	Kapton Window Thickness, cm	Additional Cu Filtration, cm
1	Be	0.0018		
2	Be	0.0053	0.0013	
3	Be	0.0018	0.017	
4	Al	0.0076	0.0013	
5	Al	0.051	0.0013	
6	Cu	0.013	0.0013	
7	Cu	0.053	0.0013	
8	Cu	0.32	0.0013	
9	Pb	0.18	0.0013	
10	Pb	0.41	0.0013	0.13
11	Pb	1.3	0.0013	0.13

$$G_i = \sum_{j=1}^{N} F_j K_j T_{ij} \Delta E_j \qquad \text{Rad } (CaF_2) \tag{2}$$

where T_{ij} is the x-ray transmission of filter i at energy interval j, and K_j is the TLD conversion

$$K_j = 4.186 \times 10^5 \frac{[1-\exp(-\mu\rho t)]}{\rho t}_j \qquad \frac{\text{Rad}(CaF_2)\text{-cm}^2}{\text{cal}} \tag{3}$$

The expression $[1-\exp(-\mu\rho t)]_j$ is the TLD absorption, and ρ and t are the density and thickness of the dosimeters, respectively.

The exposed TLDs are analyzed by using a reader whose output in nanocoulombs is proportional to the x-ray dose. Therefore, it is appropriate to define a new variable, D_i (ncoul), which is proportional to G_i. This now permits one to write Eq. (2) as

$$D_i = \lambda \sum_{j=1}^{N} F_j (1-e^{-\mu\rho t})_j T_{ij} \Delta E_j \tag{4}$$

where λ includes the constants in Eq. (3) as well as the sensitivity of the crystals. The value of λ was experimentally determined by using a calibrated x-ray source.

Thus, the expression in Eq. (4) may be rewritten in matrix form as

$$\mathbf{D} = \lambda \mathbf{A}\mathbf{F} \tag{5}$$

where $\mathbf{D}$ is a vector that describes the relative response of the 11 dosimeters, and the vector $\mathbf{F}$ denotes the incident spectrum. The elements in matrix $\mathbf{A}$ are computed by using the relation

$$A_{ij} = (1-e^{-\mu\rho t})_j \; T_{ij} \; \Delta E_j \qquad (6)$$

Further details concerning the determination of the transfer matrix **A** are given in Appendix B.

IV. CALIBRATION

The relative calibration and reproducibility of the TLDs were measured by multiple exposures on a dc x-ray tube and on the RFS. A minimal filtration of 1.8×10^{-3} cm beryllium encapsulated the crystals. The RFS delivered primarily a surface dose, whereas the 100 kV x-ray tube, whose spectrum was hardened with 0.13 mm of Cu, produced a more uniform bulk dose. Successive exposures determined that the relative response was within 2% for surface and bulk doses.

The sensitivity of the TLDs was determined by exposing the dosimeters in the fixture to the radiation from the x-ray tube. Several calibration runs were made at operating parameters of 100 kV and 1 mA for a 10 min interval. The spectrum was hardened with 0.13 mm of Cu so that the spectrum and fluence could be precisely predicted.[3] For these parameters, the total fluence at a distance of 1.4 m was calculated to be 8.04×10^{-5} cal/cm^2. The constant λ was computed to be $(6.0 \pm 0.5) \times 10^7$ for three series of calibration exposures.

[3] E. Storm, H. I. Israel, and D. W. Lier, Bremsstrahlung Emission Measurement from Thick Tungsten Targets in the Energy Range 12 to 300 kV, LA-4624, Los Alamos Scientific Laboratory, Los Alamos, New Mexico, (April 1971).

V. EXPERIMENTAL RESULTS

An improvement in signal-to-noise ratio and a consequent reduction in error were obtained by averaging the data over multiple exposures. Typically, 5 to 15 exposures of the fixture by the RFS at 1.4 m were performed before the dosimeters were read. The total dose received by each TLD dosimeter was divided by the total number of exposures to obtain an average dose per shot. The data were normalized to the response of filter set No. 1, as shown in Table 2 for both aluminum and tantalum converters. Also included in the table is the relative response when irradiated by the dc x-ray tube during the calibration experiments and estimates of the uncertainty in the data. It is believed that variations in the spectrum from shot to shot accounted for this scatter in the data.

The absolute response of TLD No. 1 is shown in Table 3 for both aluminum and tantalum converters. The machine was operated at static deuterium fill pressures of 3.3 Torr; the relevant electrical parameters are shown in the table. As anticipated, the fluence from the tantalum converter was approximately four times larger because of the Z-dependence of the x-ray efficiency.

Table 2. Relative TLD Response on the RFS

Filter Index i, No.	Al Converter Response	Ta Converter Response	X-Ray Tube Response, w/0.13 mm Cu
1	1.00	1.00	1.00
2	0.92 ± 0.01	0.96 ± 0.01	1.00 ± 0.02
3	0.87 ± 0.02	0.91 ± 0.02	1.00 ± 0.02
4	0.66 ± 0.02	0.68 ± 0.02	0.97 ± 0.02
5	0.45 ± 0.01	0.46 ± 0.02	0.95 ± 0.02
6	0.099 ± 0.008	0.12 ± 0.02	0.65 ± 0.03
7	0.027 ± 0.004	0.038 ± 0.008	0.265 ± 0.001
8	0.010 ± 0.004	0.006 ± 0.001	0.0185 ± 0.0005
9	0.002 ± 0.0004	0.002 ± 0.0004	0.0008 ± 0.0002
10	0.0007 ± 0.0003	0.0007 ± 0.0003	
11	0.00005 ± 0.00002	0.00005 ± 0.00002	

Table 3. Average Response of Reference Dosimeter No. 1

Converter	Bank Capacitance, μF	Bank Voltage, kV	Bank Energy, kJ	Response, ncoul/shot
Ta	168	14	16.5	6.0 ± 1.0
	84	16	10.8	7.0 ± 0.3
Al	168	14	16.5	1.5 ± 0.5

VI. SPECTRAL CALCULATIONS

Spectra were computed for the tantalum and aluminum converters by using an operator-implemented computer routine to search for a fluence vector **F** that satisfies the measured relative response of the TLD dosimeters that are elements of the data vector **D**. Thus, a solution for Eq. (5), $\mathbf{D} = \lambda \mathbf{AF}$, was found by using the transfer matrix in Appendix B and the data in Tables 2 and 3. From Table 3, absolute responses of 7.0 ncoul/shot for tantalum and 1.5 ncoul/shot for aluminum were used as the reference data to generate the x-ray spectra of the two converters.

The computed differential fluence at 1.4 m for tantalum and aluminum converters is shown in Table 4 and Figs. 2 and 3, respectively. Included in the table is the error in the computed **D** vector values, generated by the chosen fluence vector **F**, that falls outside the experimental data range. The computer search was designed to minimize this error.

The total x-ray fluence per shot for the two spectra was computed from Eq. (1). A total fluence of 3.37×10^{-7} cal/cm^2 was calculated for the tantalum converter, whereas a smaller fluence of 8.22×10^{-8} cal/cm^2 was computed for the aluminum converter at a distance of 1.4 m.

Table 4. Computed Differential Fluence at 1.4 m from RFS

j	E_j, keV	ΔE_j, keV	Tantalum Converter $F_j \left(\frac{cal}{cm^2\text{-keV}}\right)$	Tantalum Converter Error, %	Aluminum Converter $F_j \left(\frac{cal}{cm^2\text{-keV}}\right)$	Aluminum Converter Error, %
1	1.3	0.8	2.33×10^{-9}	0.8	2.50×10^{-9}	0.6
2	2.5	1.6	2.92×10^{-9}	0	1.13×10^{-9}	0
3	5.0	3.1	3.50×10^{-9}	0.26	7.50×10^{-10}	1.4
4	9.0	5.5	3.50×10^{-9}	0	5.00×10^{-10}	1.5
5	16	10	4.67×10^{-9}	2.8	1.08×10^{-9}	4.8
6	30	20	3.50×10^{-9}	1.8	6.75×10^{-10}	2.7
7	60	38	1.93×10^{-9}	0	3.13×10^{-10}	0.03
8	110	70	5.84×10^{-10}	0	2.25×10^{-10}	0
9	210	130	3.50×10^{-10}	0	1.25×10^{-10}	0
10	400	260	9.34×10^{-11}	0	2.00×10^{-11}	0
11	750	460	0		0	

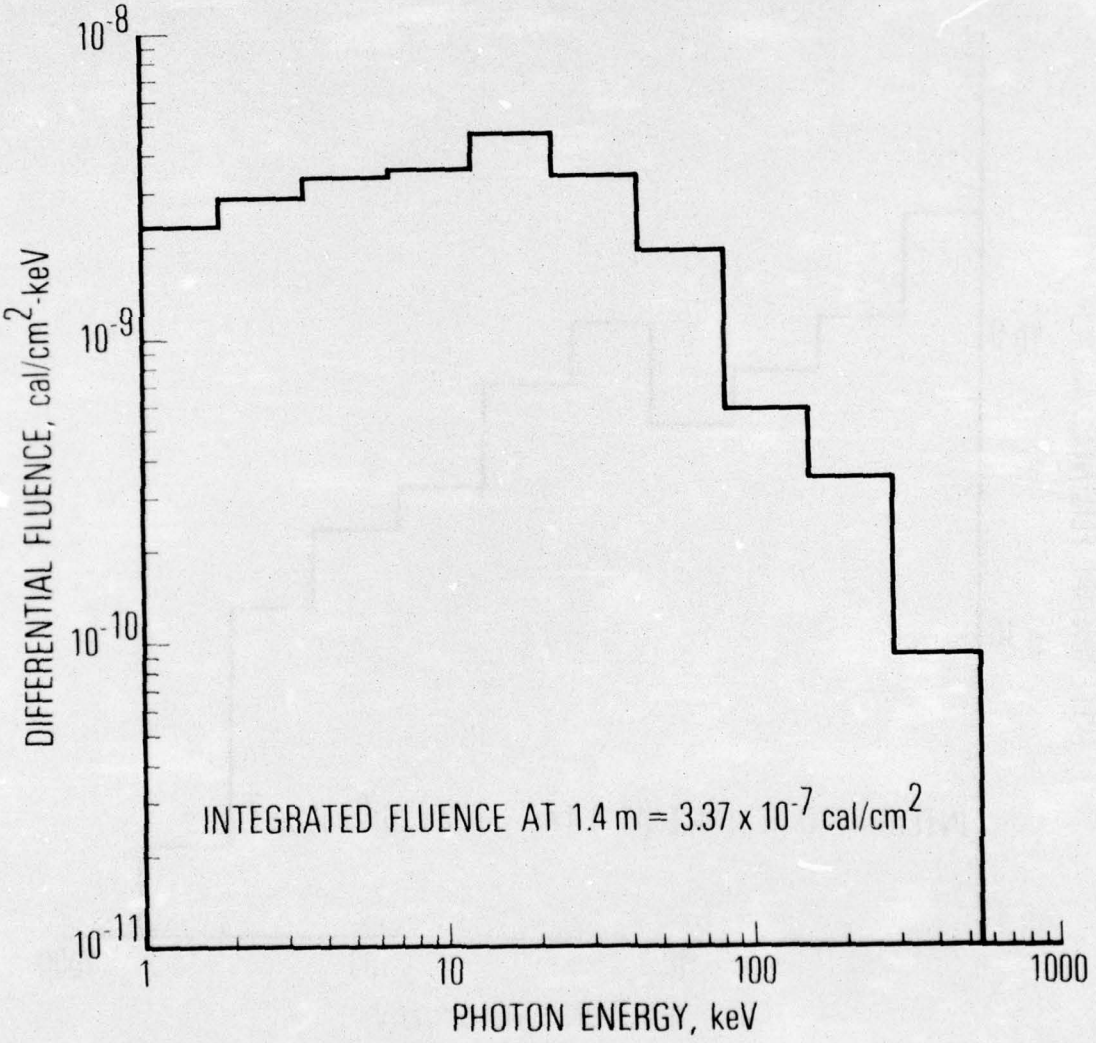

Figure 2. X-Ray Spectrum for RFS with Tantalum Converter at 1.4 m

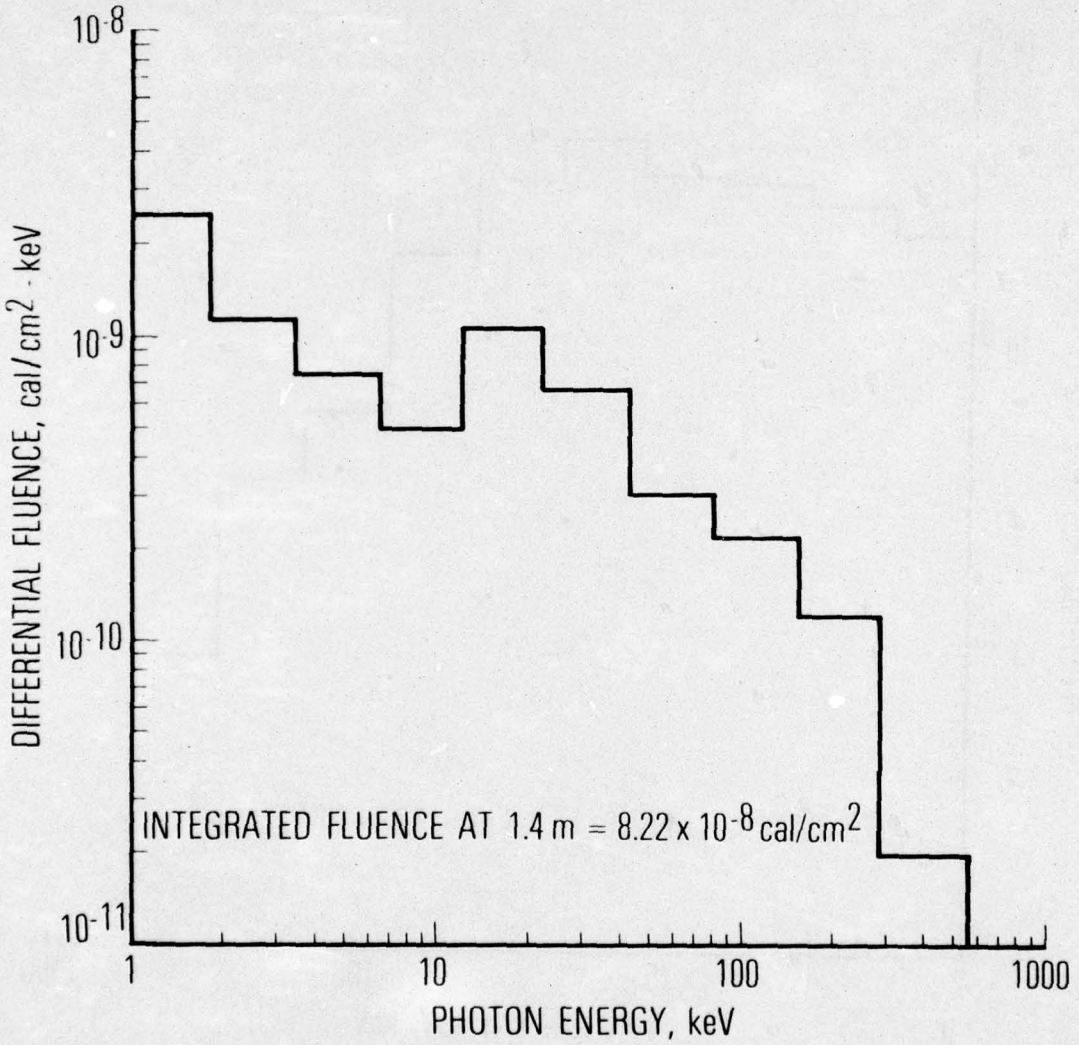

Figure 3. X-Ray Spectrum for RFS with Aluminum Converter at 1.4 m

VII. DISCUSSION

A comparison of the two spectra clearly shows the effective softening of the x-ray spectrum due to strong K-line emission at 1.5 keV when using the aluminum converter. There is also a reduction in the aluminum fluence by a factor of approximately 4 because of the Z dependence of the conversion efficiency. Other dominant features are the peak in the continuum radiation for both spectra in the 12 to 20 keV interval and the existence of hard x rays extending to energies in the hundreds of kilovolts. As expected, both spectra decrease similarly for energies greater than 80 keV ($\sim E^{-1.5}$). As indicated in Fig. 2, significant contribution from the tantalum K-line was not observed.

The spectrum for the aluminum converter was found to be similar to that of an analysis using foil-PIN diode arrays. This initial study identified the peak in the continuum at 20 to 30 keV, which is slightly greater than shown here, and the dependence of the spectra with energy was found to fall off somewhat faster ($\sim E^{-2}$). However, it is believed that the spectrum shown in Fig. 3 is the more accurate of the two because contributions from fluorescence and Compton scattering were not included in the PIN diode analysis.

Efforts were made to estimate the uncertainty in total x-ray fluence by comparing the total fluence measured in this analysis, using the TLDs and the aluminum converter, with the total flux computed in the PIN diode analysis. From this comparison, it was concluded that the x-ray pulse must be 3 to 4 nsec wide, which is approximately a factor of 5 less than measured. This discrepancy results from a combination of several factors. A factor of 2 to 3 occurs because this study analyzed an average shot from the RFS, whereas only good shots were considered in the PIN diode analysis. Another major source of error in determining absolute fluence is the uncertainty of the x-ray intensity of the dc x-ray tube used to calibrate the system.

APPENDIX A. DESCRIPTION OF FOIL-TLD DOSIMETER FIXTURE

The fixture that houses the 11 TLD dosimeters is shown in Figs. A-1 and A-2. A description of the geometry for one filter-TLD pair is also shown in Fig. A-2. The individual TLDs are sandwiched between a 0.013 mm foil of Kapton and a removable cover secured with thumbscrews located at the back plane, except for the channels that have minimal filtration. For these channels, 0.018 mm of beryllium was substituted, and the attenuation was included in the analysis.

The transmission filters on the front of the package are mounted over 8-mm-diam apertures in a 1.3-cm-thick lead plate. The relevant dimensions were selected such that an 8.6-mm-diam disk would be irradiated at the detector plane by a point source located 1.4 m from the fixture. This design ensures that each TLD is uniformly irradiated, inasmuch as the TLDs are 3.2 mm square, and avoids cross-talk between adjacent detectors (minimum TLD spacing is 1.5 cm, center-to-center).

The fixture was designed to minimize contributions from fluorescence and Compton scattering. An estimated reduction in the fluorescence from the filters by a factor of 1500 was obtained by the 11.3 cm separation of the dosimeters from the filter plane due to the isotropy of the fluorescent radiation. This feature, together with the use of lead, also reduces the effects of Compton scattering. Despite these precautions, Compton scattering introduced a significant error into the three most highly filtered TLD dosimeters. This difficulty was overcome by locating these dosimeters in three separate 2-cm-thick lead housings that were placed the same distance from the x-ray converter as the fixture.

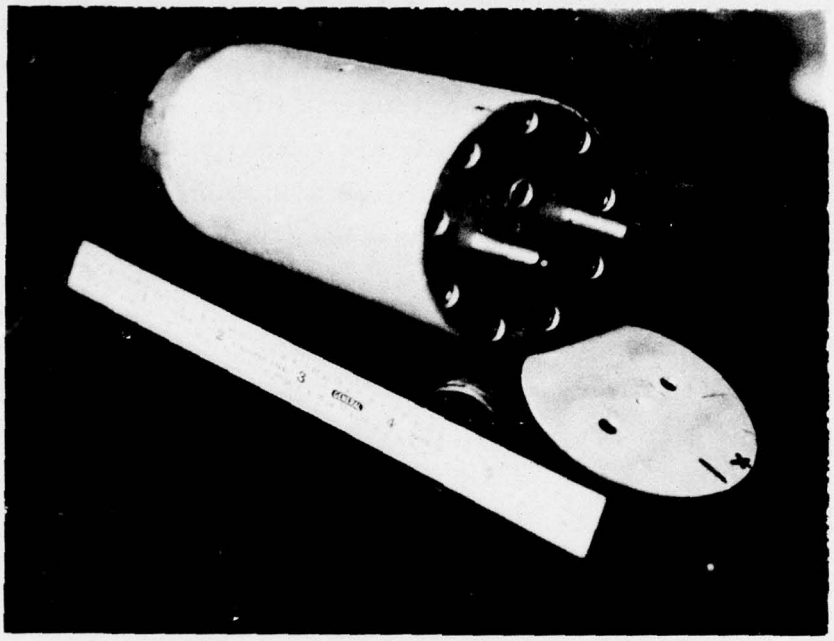

Figure A-1. TLD Dosimeter Fixture

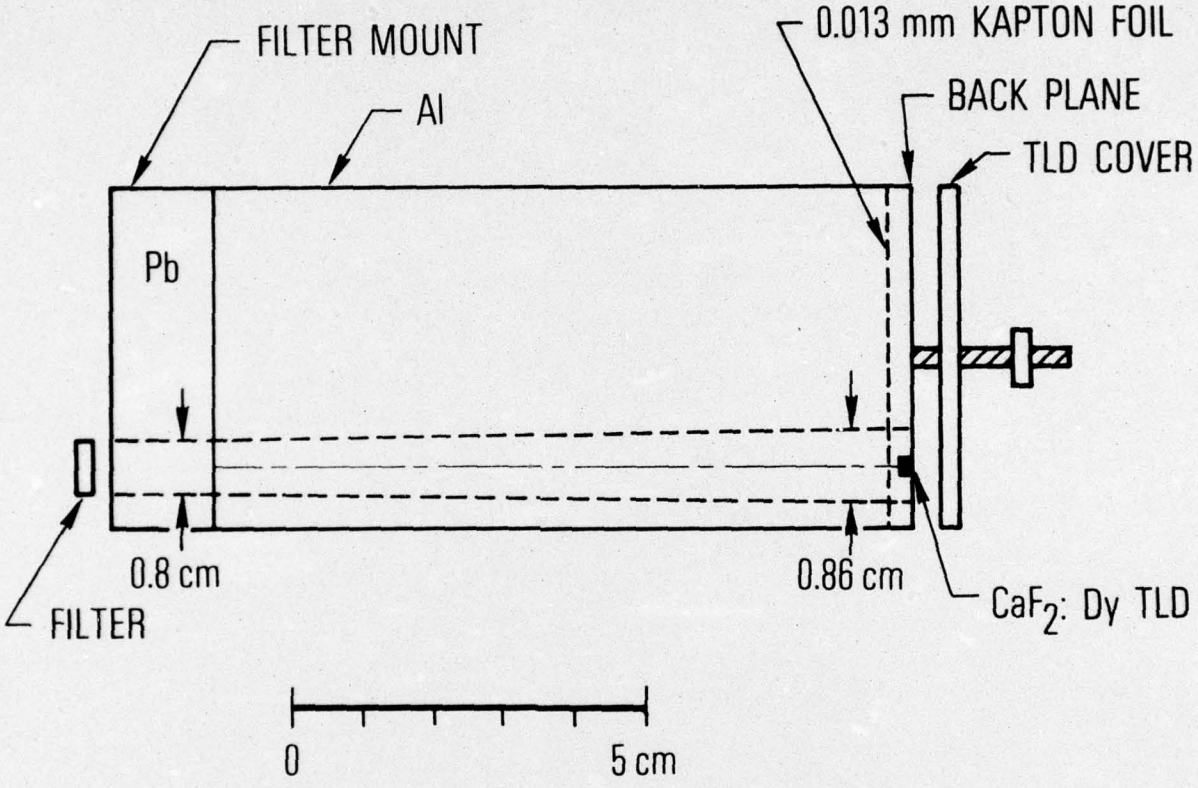

Figure A-2. TLD Dosimeter Fixture with Typical Filter-TLD Pair Shown

APPENDIX B. DETERMINATION OF TRANSFER MATRIX

The elements of the transfer matrix **A** used in the solution of Eq. (5) were computed by using the data in Figs. B-1 and B-2 and the equation

$$A_{ij} = (1-e^{-\mu\rho t})_j \, T_{ij} \, \Delta E_j \qquad \text{(B-1)}$$

where ΔE_j is the width of the jth energy interval in keV, and T_{ij} represents the transmission of foil i in interval j. The expression $(1-e^{-\mu\rho t})_j$ is the absorption of the TLD detectors.

The x-ray absorption of the TLD crystals, calculated by using the photoelectric cross section and the Klein-Nishina contribution to the energy transfer cross section, is shown in Fig. B-1 for photon energies in the range of 1 to 1000 keV. For energies less than 15 keV, the TLDs are totally absorbing. Photoelectric processes are dominant for energies as great as 150 keV, whereas absorption for energies greater than 150 keV is dominated by Compton scattering.

The x-ray transmission for each of the filters listed in Table 1 is shown in Fig. B-2, where each curve is distinguished by the same index designations used in Table 1. These transmissions were computed by using total cross sections, which consist of the photoelectric and the total Klein-Nishina cross sections. In order to avoid discontinuties, the filters were selected such that the useful spectral range of the material was significantly above the K-edge. The 11 intervals into which the spectral range 1 to 1000 keV was divided are also shown in Fig. B-2. The intervals were selected to be approximately equally spaced on a logarithmic scale. The average energy assigned to each interval E_j is shown as a subdivision and is the geometric mean of the boundaries of that interval. The transmission T_{ij} of a foil i, in the interval j, was calculated by using the average energy of that interval E_j. The computed transfer matrix **A** is shown in Table B-1.

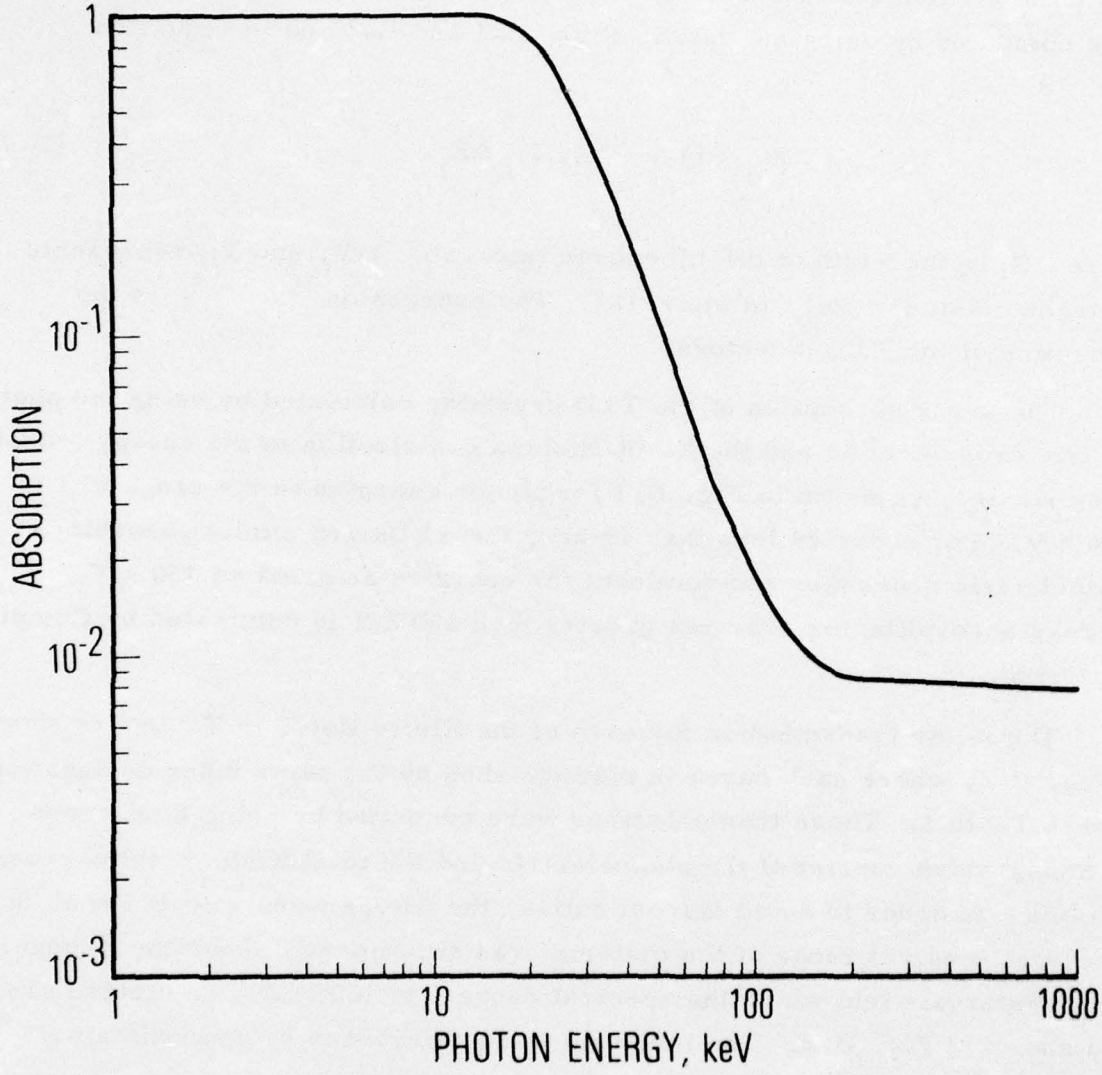

Figure B-1. X-Ray Absorption of CaF_2 TLD Dosimeters Doped with Dysprosium

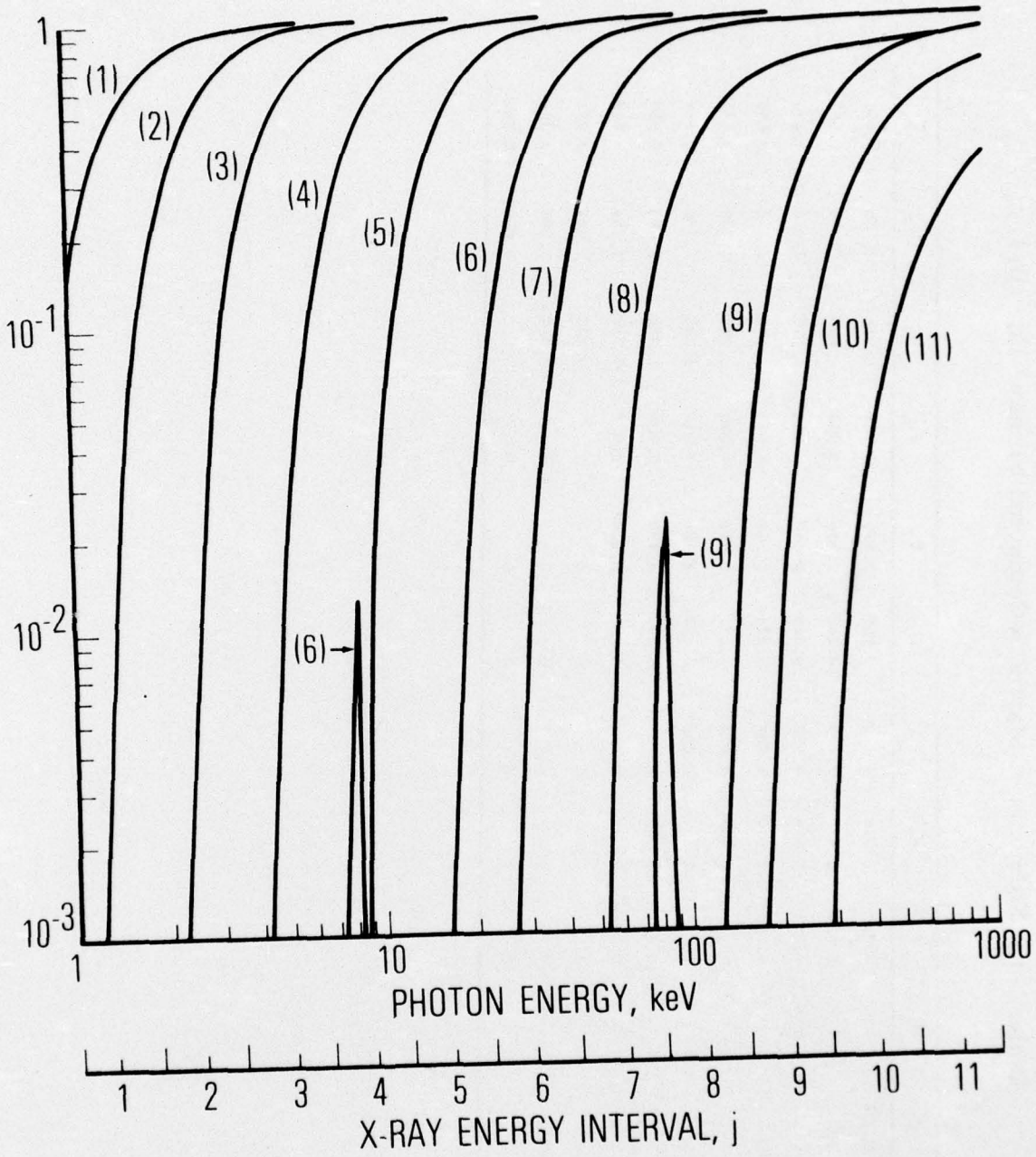

Figure B-2. X-Ray Transmission of the Filter Sets Described in Table 1 and Corresponding Energy Intervals

Table B-1. Elements of Matrix **A** Computed by using Eq. (B-1)

	F_1	F_2	F_3	F_4	F_5	F_6	F_7	F_8	F_9	F_{10}	F_{11}
D_1	0.352	1.416	3.060	5.484	9.690	8.460	2.516	1.064	1.105	2.158	3.680
D_2	0.0026	0.776	2.852	5.418	9.603	8.460	2.516	1.064	1.105	2.158	3.680
D_3	0	0.008	1.733	5.005	9.555	8.375	2.516	1.064	1.105	2.158	3.680
D_4	0	0	0.051	2.613	8.488	8.274	2.501	1.061	1.105	2.158	3.680
D_5	0	0	0	0.030	4.074	7.267	2.420	1.040	1.087	2.130	3.643
D_6	0	0	0	0	0.0087	2.479	2.106	1.016	1.086	2.136	3.654
D_7	0	0	0	0	0	0.045	1.190	0.904	1.028	2.065	3.559
D_8	0	0	0	0	0	0	0.0287	0.367	0.718	1.655	3.018
D_9	0	0	0	0	0	0	0	0	0.177	1.347	2.981
D_{10}	0	0	0	0	0	0	0	0	0.0243	0.680	2.208
D_{11}	0	0	0	0	0	0	0	0	0	0.0729	0.994

THE IVAN A. GETTING LABORATORIES

The Laboratory Operations of The Aerospace Corporation is conducting experimental and theoretical investigations necessary for the evaluation and application of scientific advances to new military concepts and systems. Versatility and flexibility have been developed to a high degree by the laboratory personnel in dealing with the many problems encountered in the nation's rapidly developing space and missile systems. Expertise in the latest scientific developments is vital to the accomplishment of tasks related to these problems. The laboratories that contribute to this research are:

Aerophysics Laboratory: Launch and reentry aerodynamics, heat transfer, reentry physics, chemical kinetics, structural mechanics, flight dynamics, atmospheric pollution, and high-power gas lasers.

Chemistry and Physics Laboratory: Atmospheric reactions and atmospheric optics, chemical reactions in polluted atmospheres, chemical reactions of excited species in rocket plumes, chemical thermodynamics, plasma and laser-induced reactions, laser chemistry, propulsion chemistry, space vacuum and radiation effects on materials, lubrication and surface phenomena, photosensitive materials and sensors, high precision laser ranging, and the application of physics and chemistry to problems of law enforcement and biomedicine.

Electronics Research Laboratory: Electromagnetic theory, devices, and propagation phenomena, including plasma electromagnetics; quantum electronics, lasers, and electro-optics; communication sciences, applied electronics, semiconducting, superconducting, and crystal device physics, optical and acoustical imaging; atmospheric pollution; millimeter wave and far-infrared technology.

Materials Sciences Laboratory: Development of new materials; metal matrix composites and new forms of carbon; test and evaluation of graphite and ceramics in reentry; spacecraft materials and electronic components in nuclear weapons environment; application of fracture mechanics to stress corrosion and fatigue-induced fractures in structural metals.

Space Sciences Laboratory: Atmospheric and ionospheric physics, radiation from the atmosphere, density and composition of the atmosphere, aurorae and airglow; magnetospheric physics, cosmic rays, generation and propagation of plasma waves in the magnetosphere; solar physics, studies of solar magnetic fields; space astronomy, x-ray astronomy; the effects of nuclear explosions, magnetic storms, and solar activity on the earth's atmosphere, ionosphere, and magnetosphere; the effects of optical, electromagnetic, and particulate radiations in space on space systems.

THE AEROSPACE CORPORATION
El Segundo, California